Biointerface Research in Applied Chemistry
Open-Access Journal (ISSN: 2069-5837)

Article
Volume 13, Issue 6, 2023, 516
https://doi.org/10.33263/BRIAC136.516

DFT Study on the Electronic Structure and Optical Properties of Orthorhombic Perovskite $CsPbBr_3$ Doped with I and Cl

Amondulloi Burhonzoda [1,*]

[1] S.U.Umarov Physical-Technical Institute of National Academy of Sciences of Tajikistan;
[2] amondullo.burkhonzoda@gmail.com (A.B.);
* Correspondence: amondullo.burkhonzoda@mail.ru (A.B.);

Scopus Author ID 57210193113

Received: 4.10.2022; Accepted: 12.11.2022; Published: 4.02.2023

Abstract: $CsPbBr_3$ is one of the active elements used in solar energy. This paper presents the results of studying the structural, electronic, and optical properties of orthorhombic $CsPbBr_3$ doped with I and Cl ions by density functional theory. Calculations were carried out using the GGA-PBE and mBJ exchange-correlation potentials. The results obtained show that the band gap of $CsPbBr_3$ decreases with increasing concentration of I; however, as the concentration of doped Cl atoms increases, the band gap increases. The calculated optical constants show that $CsPbBr_{3-x}Y_x$(Y=I, Cl) are good materials for optoelectronics and suitable for solar cells.

Keywords: $CsPbBr_3$; density functional theory; electronic properties; band gap optical properties; GGA; mBJ; solar cell.

© 2022 by the authors. This article is an open-access article distributed under the terms and conditions of the Creative Commons Attribution (CC BY) license (https://creativecommons.org/licenses/by/4.0/).

1. Introduction

The global electricity demand is growing every year. Currently, no manufacturers, households, or individuals do not require electricity. People's confidence in using solar energy is growing, and there is an opinion that the energy of the future should be based on the integrated use of solar energy. In recent years, much attention has been paid to perovskites in solar cells and optoelectronics [1-10].

The first solar cells usually made based on silicon (Si) and heterostructures, had low efficiency and high cost. Therefore, high-performance solar panels are not available to everyone.

One of the most interesting materials for creating renewable energy sources is perovskites. Solar cells based on these materials are considered promising photovoltaic technologies due to their excellent energy conversion efficiency and very low material cost. The issue of increasing the efficiency of solar cells and their availability for effective practical application attracts the attention of scientists and researchers around the world.

The study and understanding of the structural, electronic, and optical properties of $CsPbBr_3$ doped with I and Cl for use in energy storage systems and solar cells are highly relevant from the point of view of fundamental research and practical applications. Perovskite materials based on $CsPbBr_3$ doped with various atoms have high functional properties and are in high demand.

2. Materials and Methods

To study the structural, electronic, and optical properties of $CsPbBr_{3-x}Y_x$ (Y=I, Cl), we perform density functional theory (DFT) simulations [11] using the full linearized potential augmented plane wave method [12] implemented in WIEN2k [13]. Structural and electronic properties of $CsPbBr_{3-x}Y_x$ (Y=I, Cl) were studied within the framework of DFT using exchange-correlation potentials GGA-PBE [14] and mBJ [15]. In all calculations, the RMT* kmax value was assumed to be 7.0. RMT values were set at 2.5 AU. for Cs, Pb, Br, I, and 2.43 a.u. for Cl. The $CsPbBr_3$ used in our calculations belongs to the orthorhombic crystal structure of the space group Pnma. Models of I and Cl doped with $CsPbBr_3$ are constructed by replacing the corresponding number of Br ions with the corresponding number of I and Cl ions.

3. Results and Discussion

3.1. Structural and electronic property.

To study the effect of doping with I and Cl on the structural, electronic, and optical properties of $CsPbBr_3$, as well as on its absorption capacity, we replaced the corresponding number of Br atoms with the corresponding I and Cl atoms with the abundance ratio of I (x = 0, 0.5, 1, 1.5) and Cl (x = 0, 0.25, 1, 1.25). The crystal structures of these materials were modeled using the 3D visualization program for electronic and structural analysis VESTA. The unit cell of each material consists of 20 atoms. The initial structure of CsPbBr3 and the crystal structure after doping with various contents of I and Cl are shown in Figures 1 and 2, respectively.

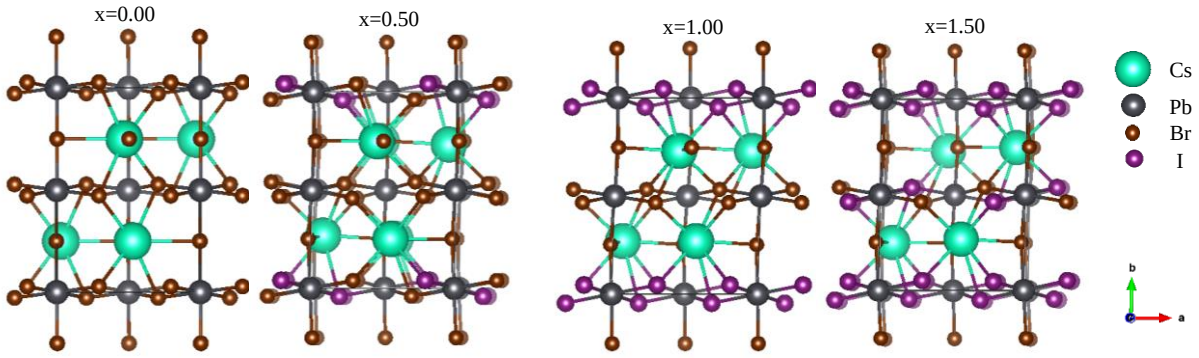

Figure 1. Atomic structures of $CsPbBr_{3-x}I_x$ at different contents of I (x = 0, 0.5, 1, 1.5).

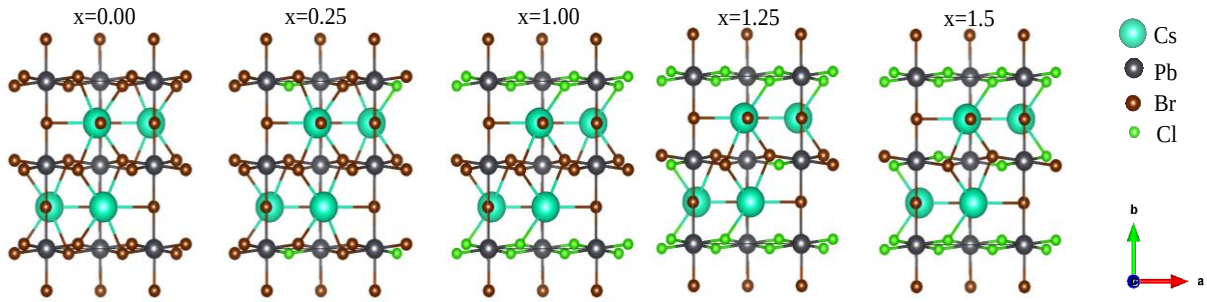

Figure 2. Atomic structures of $CsPbBr_{3-x}Cl_x$ at different Cl contents (x = 0, 0.25, 1, 1.25, 1.5).

Table 1 shows the structural parameters of $CsPbBr_{3-x}I_x$ (x = 0, 0.5, 1, 1.5) and $CsPbBr_{3-x}Cl_x$ (x = 0, 0.25, 1, 1.25) after geometric optimization. The calculated parameters and lattice volume of pure $CsPbBr_3$, given in Table 1, are in good agreement with the theoretical and experimental results [16, 17]. Thus, we can conclude that our calculated structural parameters

are correct. The results show the calculated equilibrium parameters (a, b and c, in Å) and volume (V, in Å^3) of the lattice. A graphical representation of the results of $CsPbBr_{3-x}I_x$ (x = 0, 0.5, 1, 1.5) is shown in Figure 3.

Table 1. Structural parameters of $CsPbBr_{3-x}Y_x$ (Y=I, Cl).

Lattice parameters	This work	Other
$CsPbBr_3$		
a (Å)	8,45	8.56[16], 8.25[17]
b (Å)	11,8	12.18[16], 11.75[17]
c (Å)	8,14	8.51[16], 8.20[17]
V (Å^3)	812,79	888.2[16], 795.6[17]
$CsPbBr_{2.5}I_{0.5}$		
a (Å)	8,59	
b (Å)	11,79	
c (Å)	8,31	
V (Å^3)	843,1	
$CsPbBr_2I_1$		
a (Å)	8,75	
b (Å)	11,81	
c (Å)	8,42	
V (Å^3)	870,59	
$CsPbBr_{1.5}I_{1.5}$		
a (Å)	8,92	
b (Å)	11,79	
c (Å)	8,58	
V (Å^3)	903,46	
$CsPbBr_{2.75}Cl_{0.25}$		
a (Å)	8.42	
b (Å)	11.87	
c (Å)	8.18	
V (Å^3)	819.13	
$CsPbBr_2Cl_1$		
a (Å)	8.19	
b (Å)	11.91	
c (Å)	8.03	
V (Å^3)	784.27	
$CsPbBr_{1.75}Cl_{1.25}$		
a (Å)	8.14	
b (Å)	11.90	
c (Å)	7.97	
V (Å^3)	773.12	
$CsPbBr_{1.5}Cl_{1.5}$		
a (Å)	8.07	
b (Å)	11.90	
c (Å)	7.95	
V (Å^3)	764.14	

The results show that with an increase in the concentration of I atoms, the geometric parameters of $CsPbBr_{3-x}I_x$ noticeably change. In this case, the parameters a, b, and the volume of the crystal lattice increase linearly. The empirical formulas a = 0.314x + 8.442, c = 0.286x + 8.148, and V = 59.9x + 812.56, respectively, express the change in parameters *a*, *c*, and the *volume* of the crystal lattice of $CsPbBr_{3-x}I_x$. The change in parameter *b* does not obey a linear law and, in turn, changes little.

Structural analysis of $CsPbBr_{3-x}Cl_x$ shows that the lattice constants of the unit cell change noticeably with an increase in the concentration of doped Cl atoms. As shown in Figure 4, in contrast to I doped with $CsPbBr_3$, with an increase in the Cl(x) content, the size of the

elementary cell decreases proportionally from 0.25 to 1.5 according to the function V(x) = -44.569x + 829.73(Å)^3.

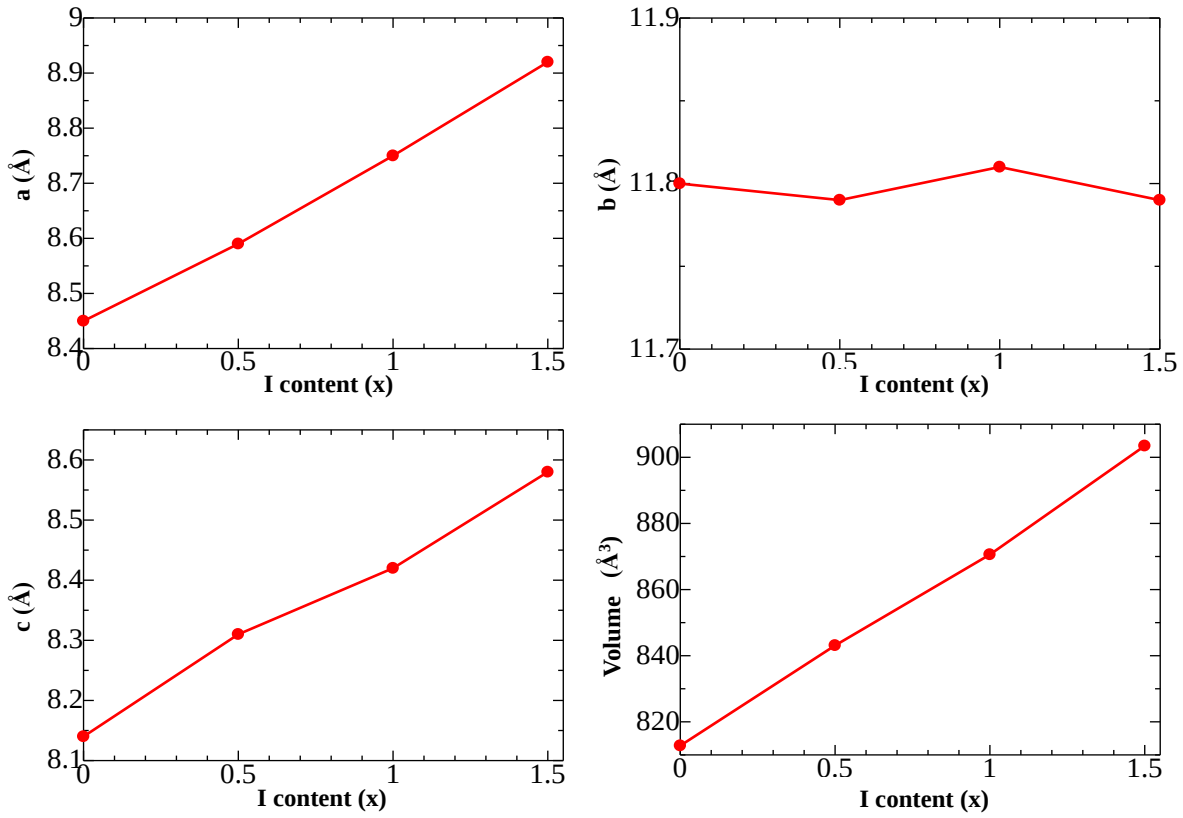

Figure 3. Dependences of the lattice parameters of $CsPbBr_{3-x}I_x$ on the content of I atoms.

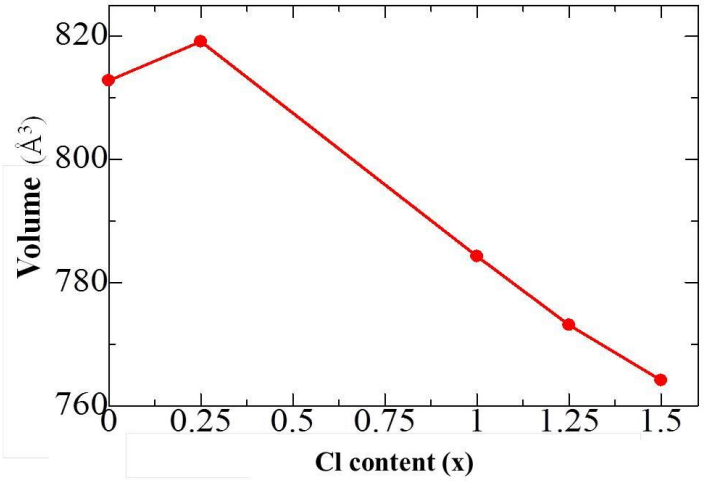

Figure 4. Unit cell volume depends on the content of Cl(x).

Below, we present the results of studying the electronic properties of $CsPbBr_{3-x}I_x$ and $CsPbBr_{3-x}Cl_x$. To obtain additional information about the electronic structure and a comprehensive understanding of the band gap energy, quantum mechanical calculations of the electronic structure of $CsPbBr_{3-x}I_x$ and $CsPbBr_{3-x}Cl_x$ were carried out. The electronic properties of these structures are obtained by studying the density of electronic states. The density of electronic states of $CsPbBr_{3-x}I_x$ and $CsPbBr_{3-x}Cl_x$ was calculated by the LAPW method [18] and is shown in Figures 5 and 6, respectively. Analyzing the state density, we noticed a change in the band gap with a change in the content of I and Cl. Figure 5 shows the results of quantum mechanical calculations of $CsPbBr_{3-x}I_x$(x = 0, 0.5, 1, 1.5) within the GGA

and mBJ approximations. The distributions of the density of states are built in the range from -4 to 4 eV.

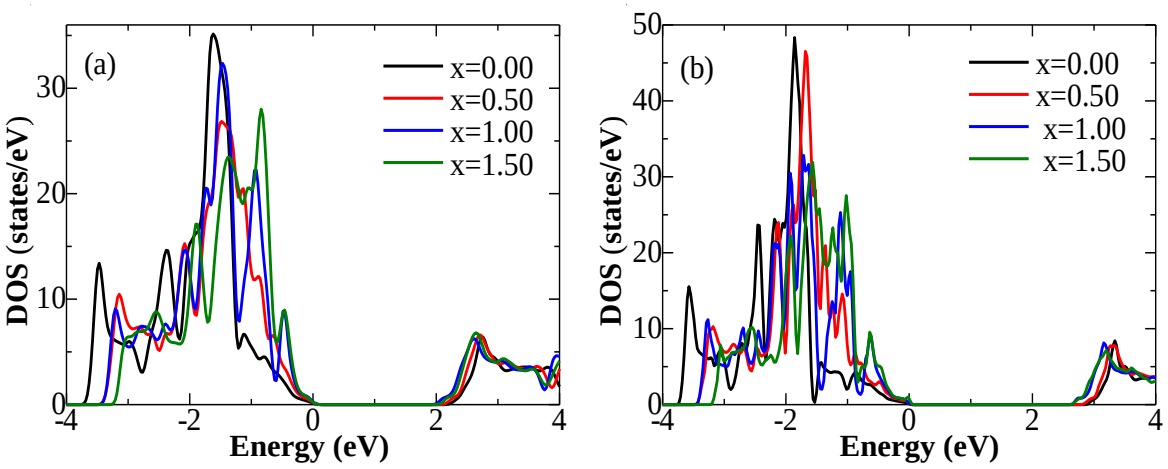

Figure 5. The density of state of $CsPbBr_{3-x}I_x$ (x = 0, 0.5, 1, 1.5 as a function of energy in the GGA **(a)** and mBJ **(b)** approximations.

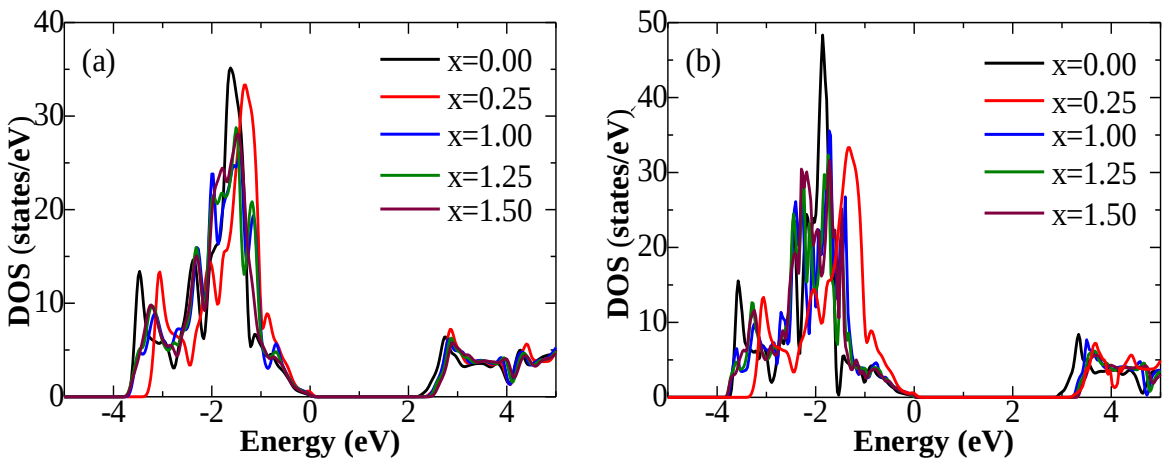

Figure 6. The density of state of $CsPbBr_{3-x}Cl_x$ (x = 0, 0.25, 1, 1.25, 1.5) as a function of energy in the GGA **(a)** and mBJ **(b)** approximations.

The band gaps of $CsPbBr_{3-x}I_x$ and $CsPbBr_{3-x}Cl_x$ calculated using the GGA and mBJ potentials are given in Table 2. The results show that the band gap of $CsPbBr_{3-x}I_x$ decreases with increasing concentration of doped I atoms. In contrast to I doped with $CsPbBr_3$, with an increase in the Cl concentration in the composition of $CsPbBr_3$, the band gap increases accordingly. The band gap value calculated using the mBJ potential is larger than that obtained using the GGA potential.

Table 2. Band gaps of $CsPbBr_{3-x}I_x$ (x = 0, 0.5, 1, 1.5) and $CsPbBr_{3-x}Cl_x$ (x = 0, 0.25, 1, 1.25, 1.5) calculated using the GGA and mBJ potentials.

System	This work		Other works (эВ)
	GGA(эВ)	mBJ(эВ)	
$CsPbBr_3$	2,27	3,06	2.89[19], 2,22[20], 2,29[21]
$CsPbBr_{2.5}I_{0.5}$	1.99	2.75	
$CsPbBr_2I_1$	1.90	2.61	
$CsPbBr_{1.5}I_{1.5}$	1.86	2.57	
$CsPbBr_{2.75}Cl_{0.25}$	2,32	3,20	
$CsPbBr_2Cl_1$	2,35	3,23	

System	This work		Other works (эВ)
	GGA(эВ)	mBJ(эВ)	
$CsPbBr_{1.75}Cl_{1.25}$	2,40	3,28	
$CsPbBr_{1.5}Cl_{1.5}$	2,42	3,34	

Figures 7 and 8, respectively, show the dependence of the $CsPbBr_3$ band gap on the concentration of doped I and Cl atoms. The empirical formulas bg=-0.162x+2.084 and bg=-0.19x+2.835 express the change in the band gap of $CsPbBr_{3-x}I_x$ in GGA and mBJ calculations, respectively. Using these equations, one can estimate the band gap in $CsPbBr_{3-x}I_x$ for any concentration I.

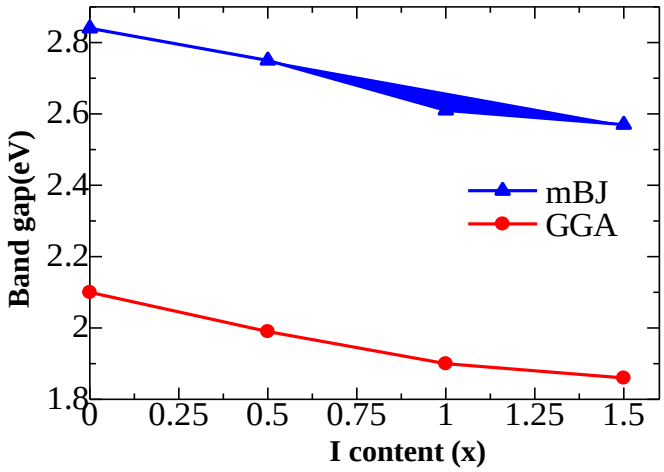

Figure 7. Band gap at various concentration ratios of I doped in $CsPbBr_3$.

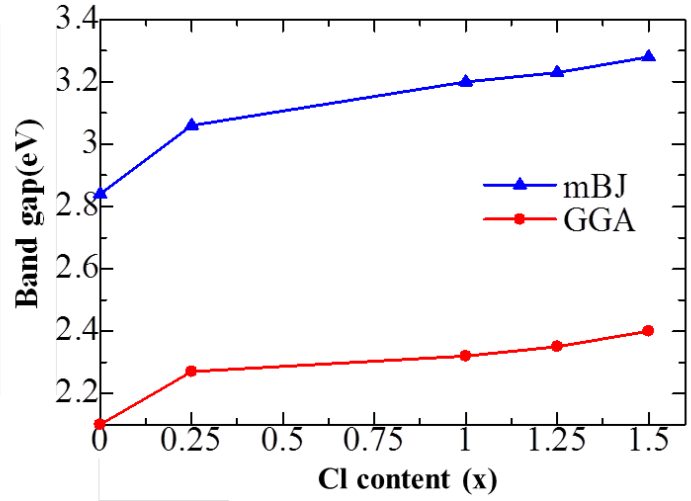

Figure 8. Band gap at various concentration ratios of Cl doped in $CsPbBr_3$.

3.1. Optical property.

The study of the optical properties of these perovskites is of great importance in connection with the possibility of their use in solar cells [22–27]. Typically, the optical properties of these compounds are studied using parameters such as absorption coefficient, optical conductivity, refractive index, and reflectance, which can be calculated from the equations [28-32]:

$$\alpha(\omega) = \sqrt{2\omega}\sqrt{\sqrt{\varepsilon_1^2(\omega)+\varepsilon_2^2(\omega)}-\varepsilon_1(\omega)} \quad (1)$$

$$\sigma(\omega) = \frac{i\omega}{4\pi}\varepsilon(\omega) \quad (2)$$

$$n(\omega) = \frac{1}{\sqrt{2}}\sqrt{\sqrt{\varepsilon_1^2(\omega)+\varepsilon_2^2(\omega)}+\varepsilon_1(\omega)} \quad (3)$$

$$R(\omega) = \left|\frac{\sqrt{\varepsilon(\omega)-1}}{\sqrt{\varepsilon(\omega)+1}}\right|^2 \quad (4)$$

где $\varepsilon(\omega) = \varepsilon_1(\omega) + i\varepsilon_2(\omega)$

If you calculate a complex dielectric function, then you can easily study all the other optical properties of perovskite materials. As is known, the permittivity consists of two parts: the real part $\varepsilon_1(\omega)$ and the imaginary part $\varepsilon_2(\omega)$. $\varepsilon_1(\omega)$ is the accumulated energy available for issuing. $\varepsilon_2(\omega)$ explains the absorption capacity and behavior of these materials. Figures 9 and 10 show the real $\varepsilon_1(\omega)$ and imaginary $\varepsilon_2(\omega)$ parts of the permittivity of $CsPbBr_{3-x}I_x$ and $CsPbBr_{3-x}Cl_x$ depending on the photon energy in the framework of quantum chemical calculations, respectively.

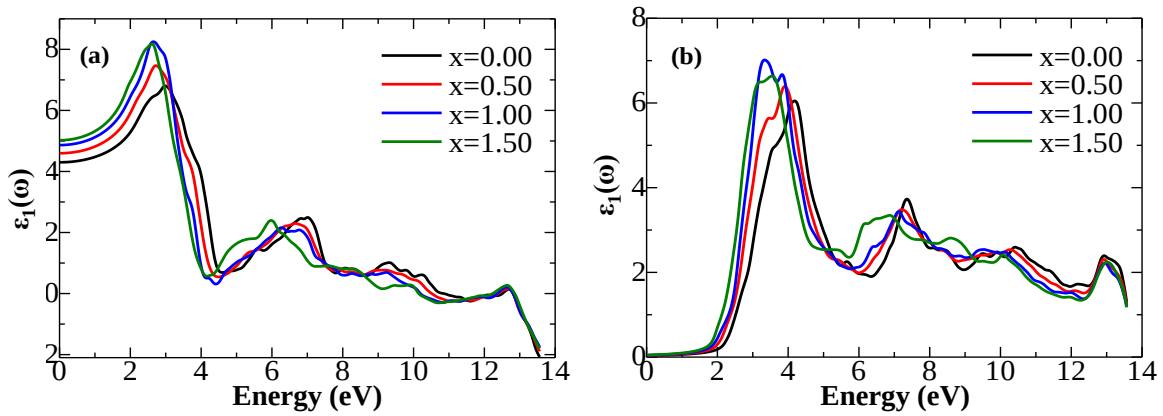

Figure 9. Calculated **(a)** values of $\varepsilon_1(\omega)$ and **(b)** values of $\varepsilon_2(\omega)$ of $CsPbBr_{3-x}I_x$ (x = 0, 0.25, 1, 1.25, 1.5) depending on the energy using the GGA potential.

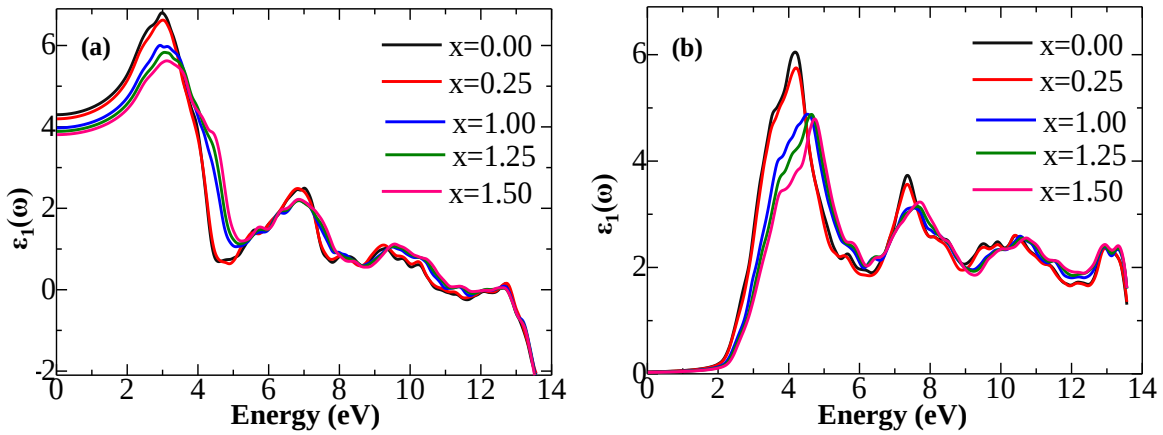

Figure 10. Calculated **(a)** values of $\varepsilon_1(\omega)$ and **(b)** values of $\varepsilon_2(\omega)$ of $CsPbBr_{3-x}Cl_x$ (x = 0, 0.25, 1, 1.25, 1.5) depending on the energy using the GGA potential.

$\varepsilon_1(\omega)$ is the reserve energy of the medium or material that can be given away. Figure 9(a) shows that at sufficiently high energies, $CsPbBr_{3-x}I_x$ exhibits metallic behavior. The value of $\varepsilon 1(\omega)$ increases in the range of 0–3 eV and reaches its maximum value in the region of 3 eV. It can be seen that with a further increase in the photon energy, the value of $\varepsilon_1(\omega)$ begins to

take negative values beyond 10 eV. These negative values explain that in this range, the $CsPbBr_{3-x}I_x$ compounds will behave like a metal, having a high reflectivity of the light incident.

$\varepsilon_2(\omega)$ explains the absorption capacity and behavior of these materials. The imaginary part of the permittivity (ε_2) is zero at 0 eV in the case of a pure system. This means there is no energy absorption in $CsPbBr_3$, in contrast to iodine-doped perovskite CsPbBr3, where a positive value of ε2 is observed. As can be seen from Figure 9(b), the absorption capacity of $CsPbBr_3$, $CsPbBr_{2.5}I_{0.5}$, $CsPbBr_2I_1$, and $CsPbBr_{1.5}I_{1.5}$ increases to maximum values of 4.17, 3.9, 3.33 and 3.6 at 6.05, 6.39, 7.02 and 6.6 eV, respectively. Then the values of $\varepsilon_2(\omega)$ rapidly decrease for all compounds. These systems showed a noticeable peak around 3 eV with non-zero absorption even at 0 eV. It should be noted that with an increase in the concentration of doped iodine ions, the absorption capacity of CsPbBr3 increases accordingly. A shift of the absorption peaks towards low energies is also observed. The absorption edge of iodine-doped $CsPbBr_3$ is observed towards lower energies (0.2 eV). The increase in absorption can be explained by a decrease in the band gap, as can be seen in Figure 7.

Figure 10 (a) shows that the value of $\varepsilon1(\omega)$ of $CsPbBr_{3-x}Cl_x$ increases in the range of 0–3 eV and reaches its maximum value in the region of 3 eV. Then it decreases and becomes negative at high energies (12 eV and above). The imaginary part $\varepsilon_2(\omega)$ is related to the band gap energy. Figure 10(b) shows that $CsPbBr_3$ has the highest peaks in the visible and infrared regions due to the smaller band gap compared to other compounds.

Given the values of the real $\varepsilon_1(\omega)$ and imaginary $\varepsilon_2(\omega)$ parts of the permittivity, optical properties such as absorption coefficient $\alpha(\omega)$, optical conductivity spectra $\sigma(\omega)$, refractive index $n(\omega)$ and reflection coefficient $R(\omega)$, which characterizes the interaction of light with matter, is determined by equations (1-4). Figure 11 shows the dependence of the absorption coefficient spectra, optical conductivity spectra, and refractive and reflection indices on the energy of $CsPbBr_{3-x}I_x$.

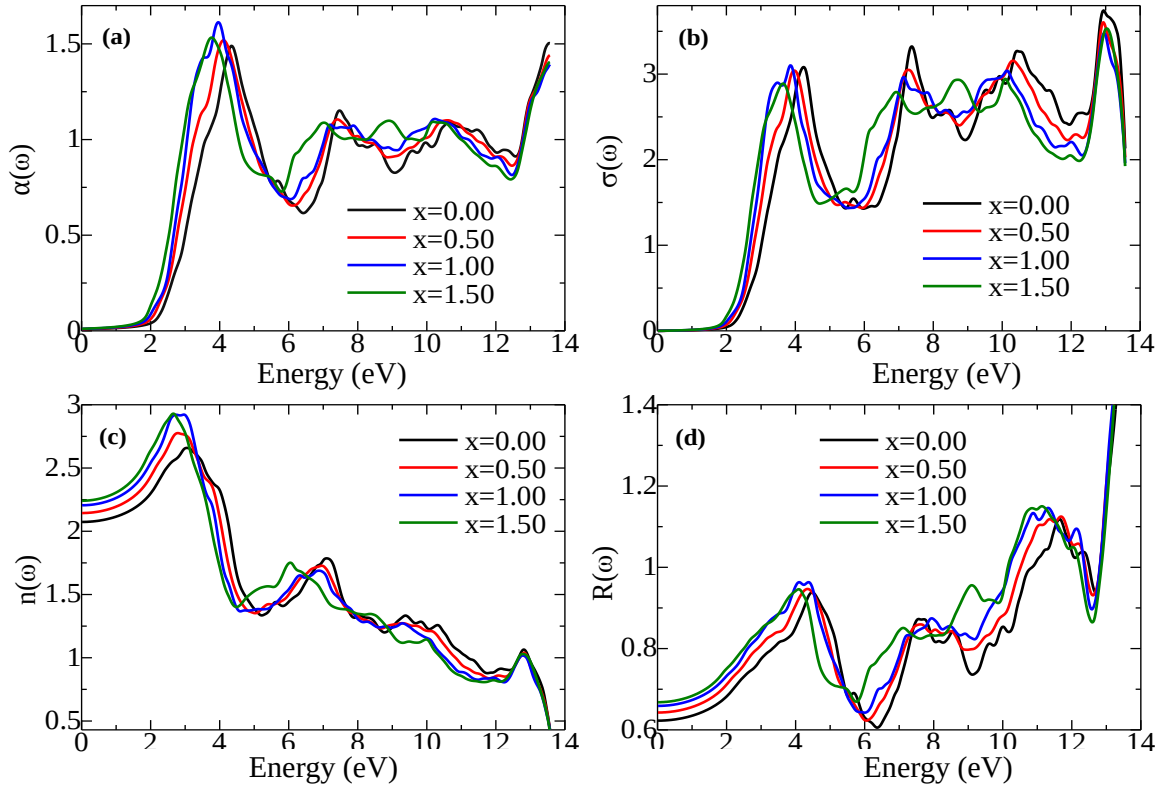

Figure 11. Calculated **(a)** absorption coefficient spectra α(ω), **(b)** optical conductivity spectra σ(ω), **(c)** refractive index n(ω), **(d)** reflection coefficient R(ω) of $CsPbBr_{3-x}I_x$ perovskite using the GGA potential.

As can be seen from Figure 11(a), the influence of doping changes the absorption spectra. The absorption threshold increases at 1.8, 1.4, 1.2, and 0.95 eV and reaches a maximum value of 1.39, 1.52, 1.62, and 1.53 at 4.34, 4.14, 3 .95 and 3.76 eV for $CsPbBr_3$, $CsPbBr_{2.5}I_{0.5}$, $CsPbBr_2I_1$, and $CsPbBr_{1.5}I_{1.5}$, respectively.

The optical conductivity spectrum σ(ω) is shown in Figure 11(b), which gives an idea of the conductivity of a perovskite compound under optical excitation caused by penetrating photon energy beams. Figure 11(d) shows that the optical conductivity has a zero value in the visible region up to about 2 eV and tends to increase in the limit up to 4 eV and reaches higher values in the UV range. The optical conductivity increases accordingly with an increase in the concentration of I in the $CsPbBr_3$ structure. The minimum σ(ω) in the low energy region and the corresponding zero values in the emitted region show that the incident light in this energy region cannot cause optical excitations for these compounds.

The calculated refractive index (n) for $CsPbBr_3$, $CsPbBr_{2.5}I_{0.5}$, $CsPbBr_2I_1$, and $CsPbBr_{1.5}I_{1.5}$ is 2.07, 2.14, 2.20, and 2.24, respectively. As shown in Figure 11(c), the refractive index increases in the range of 0-3 eV and reaches its maximum value in the vicinity of 3 eV. Then it decreases and tends to zero at high energies for all compounds. The n(ω) spectrum is very similar to the spectrum of $\varepsilon_1(\omega)$.

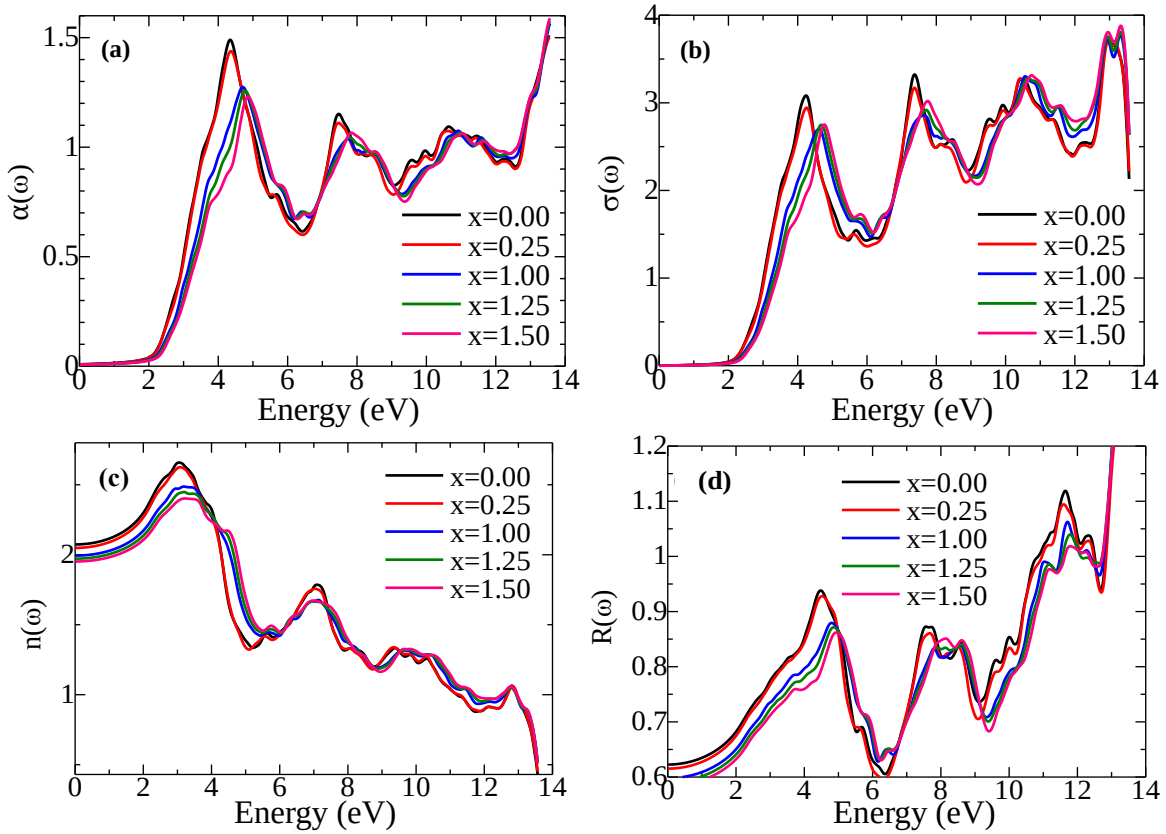

Figure 12. Calculated **(a)** absorption coefficient spectra α(ω), **(b)** optical conductivity spectra σ (ω), **(c)** refractive index n(ω), **(d)** reflection coefficient R(ω) of $CsPbBr_{3-x}Cl_x$ perovskite using the GGA potential.

Figure 12(a) shows the absorption spectra of $CsPbBr_{3-x}Cl_x$ (x = 0, 0.25, 1, 1.25, 1.5). $CsPbBr_{2.75}Cl_{0.25}$ has better absorption characteristics and great potential as a photovoltaic conversion material for perovskite solar cells.

Figure 12(b) shows the optical conductivity spectra of the $CsPbBr_{3-x}Cl_x$ (x = 0, 0.25, 1, 1.25, 1.5) system depending on the energy range from 0 to 14 eV. We used formula (2) to calculate σ(ω). Within the framework of GGA calculations, the optical conductivity of CsPbBr3 perovskite takes the form of a zero value for energies up to 2 eV, starting from 2 eV,

increases and reaches a maximum at 4.77 eV, and then sharply drops to 1.36, after 6 eV it again tends to increase. Optical conductivity for other compounds of the $CsPbBr_{3-x}Cl_x$ system has a similar trend.

Figure 12(c) shows the calculated refractive index versus energy. For $CsPbBr_{3-x}Cl_x$ (x = 0, 0.25, 1, 1.25, 1.5), in the framework of GGA calculations, the refractive index rises to the maximum values of 2.65, 2.62, 2.48, 2.44, and 2.40 at 3.03, 3.11, 3.19, 3.19, and 3.22 eV, respectively. The figure shows that at energies greater than 12.96 eV for all compounds, the refractive index tends to 0.

As can be seen from Figure 12(d), the reflectance for CsPbBr3 starts to increase from R(0)=0.6226 to 0.90 at 4.77 eV and then decreases to 0.60 at about 6.35 eV. The reflection coefficient again starts to increase from 6.4 eV. A similar trend has a reflection coefficient for other compounds of the $CsPbBr_{3-x}Cl_x$ system

4. Conclusions

Structural, electronic, and optical properties of $CsPbBr_{3-x}Y_x$ (Y=I, Cl) have been studied using quantum mechanical calculations. The results obtained showed that the band gap of $CsPbBr_3$ decreases with increasing concentration of I; however, as the concentration of doped Cl atoms increases, the band gap increases. The calculated optical properties, consisting of the dielectric function, absorption coefficient spectra, optical conductivity spectra, refractive index, and reflectance, showed that I doped with $CsPbBr_3$, compared to undoped CsPbBr3, has a high absorption coefficient. The high absorption power and direct band gap over a wide range show that $CsPbBr_{3-x}Y_x$ (Y=I, Cl) is suitable for use in solar cells. The calculated optical constants of $CsPbBr_{3-x}Y_x$ (Y=I, Cl) perovskites show that they are good materials for use in optoelectronics. Notably, $CsPbBr_{3-x}Y_x$ (Y=I) exhibits the strongest absorption in the visible light range, the highest number of absorbing photons, and a suitable band gap. Our study provides a theoretical justification for creating highly efficient photovoltaic devices based on $CsPbBr_{3-x}Y_x$ (Y=I, Cl) and synthesizing photovoltaic materials with improved characteristics.

The application of DFT to study the optoelectronic properties of functional materials proves that this method is an important computational tool for studying fundamental principles of materials and plays a decisive role in clarifying their functionality [35-46].

Funding

This research was funded by the International Innovation Center for Nanotechnologies of the CIS (ICNTC CIS) and the Interstate Fund for Humanitarian Cooperation of the CIS Member States (IFGS)., grant number 22-112".

Acknowledgments

This work was carried out within the framework of the activities of the ICNTC CIS with the support of the IFGS and the Joint Institute for Nuclear Research.

Conflicts of Interest

The funders had no role in the design of the study; in the collection, analyses, or interpretation of data; in the writing of the manuscript, or in the decision to publish the results.

References

1. Jeon, N. J.; Noh, J. H.; Yang, W. S.; Kim, Y. C.; Ryu, S.;, Seo, J.; & Seok, S. il. Compositional engineering of perovskite materials for high-performance solar cells. *Nature* **2015**, *517*, 476–480, https://doi.org/10.1038/nature14133.
2. Eperon, G. E.; Paternò, G. M.; Sutton, R. J.; Zampetti, A.; Haghighirad, A. A.; Cacialli, F.; & Snaith, H. J. Inorganic caesium lead iodide perovskite solar cells. *Journal of Materials Chemistry A* **2015**, *3*, 19688–19695, https://doi.org/10.1039/C5TA06398A
3. Sutton, R. J.; Eperon, G. E.; Miranda, L.; Parrott, E. S.; Kamino, B. A.; Patel, J. B.; Hörantner, M. T.; Johnston, M. B.; Haghighirad, A. A.; Moore, D. T.; & Snaith, H. J. Bandgap-Tunable Cesium Lead Halide Perovskites with High Thermal Stability for Efficient Solar Cells. *Advanced Energy Materials* **2016**, *6*, 1502458, https://doi.org/10.1002/aenm.201502458
4. Swarnkar, A.; Marshall, A. R.; Sanehira, E. M.; Chernomordik, B. D.; Moore, D. T.; Christians, J. A.; Chakrabarti, T.; & Luther, J. M. Quantum dot–induced phase stabilization of α-$CsPbI_3$ perovskite for high-efficiency photovoltaics. *Science* **2016**, *354*, 92–95, https://doi.org/10.1126/science.aag2700
5. Hu, Y.; Bai, F.; Liu, X.; Ji, Q.; Miao, X.; Qiu, T.; & Zhang, S. Bismuth Incorporation Stabilized α-$CsPbI_3$ for Fully Inorganic Perovskite Solar Cells. *ACS Energy Letters* **2017**, *2*, 2219–2227, https://doi.org/10.1021/acsenergylett.7b00508
6. Luo, P.; Xia, W.; Zhou, S.; Sun, L.; Cheng, J.; Xu, C.; & Lu, Y. Solvent Engineering for Ambient-Air-Processed, Phase-Stable $CsPbI_3$ in Perovskite Solar Cells. *The Journal of Physical Chemistry Letters* **2016**, *7*, 3603–3608, https://doi.org/10.1021/acs.jpclett.6b01576
7. Marronnier, A.; Roma, G.; Boyer-Richard, S.; Pedesseau, L.; Jancu, J.-M.; Bonnassieux, Y.; Katan, C.; Stoumpos, C. C.; Kanatzidis, M. G.; & Even, J. Anharmonicity and Disorder in the Black Phases of Cesium Lead Iodide Used for Stable Inorganic Perovskite Solar Cells. *ACS Nano* **2018**, *12*, 3477–3486, https://doi.org/10.1021/acsnano.8b00267
8. Wang, Y.; Zhang, T.; Kan, M.; & Zhao, Y. Bifunctional Stabilization of All-Inorganic α-$CsPbI_3$ Perovskite for 17% Efficiency Photovoltaics. *Journal of the American Chemical Society* **2018**, *140*, 12345–12348, https://doi.org/10.1021/jacs.8b07927
9. Kulbak, M.; Gupta, S.; Kedem, N.; Levine, I.; Bendikov, T.; Hodes, G.; & Cahen, D. Cesium Enhances Long-Term Stability of Lead Bromide Perovskite-Based Solar Cells. *The Journal of Physical Chemistry Letters* **2016**, *7*, 167–172, https://doi.org/10.1021/acs.jpclett.5b02597
10. Liang, J.; Wang, C.; Wang, Y.; Xu, Z.; Lu, Z.; Ma, Y.; Zhu, H.; Hu, Y.; Xiao, C.; Yi, X.; Zhu, G.; Lv, H.; Ma, L.; Chen, T.; Tie, Z.; Jin, Z.; & Liu, J. All-Inorganic Perovskite Solar Cells. *Journal of the American Chemical Society* **2016**, *138*, 15829–15832, https://doi.org/10.1021/jacs.6b10227
11. Bagayoko, D. Understanding density functional theory (DFT) and completing it in practice. *AIP Advances* **2014**, *4*, 127104, https://doi.org/10.1063/1.4903408
12. Cottenier, S. et al. Density Functional Theory and the family of (L) APW-methods: a step-by-step introduction. *Instituut voor Kern-en Stralingsfysica, KU Leuven* **2002**, Т. 4, №. 0, С. 41,
13. Blaha, P.; Schwarz, K.; Madsen, G. K.; Kvasnicka, D.; & Luitz, J. wien2k. *An augmented plane wave+ local orbitals program for calculating crystal properties* **2001**, *60*, http://www.wien2k.at/reg_user/textbooks/DFT_and_LAPW_2nd.pdf.
14. Perdew, J. P.; & Yue, W. Accurate and simple density functional for the electronic exchange energy: Generalized gradient approximation. *Physical Review B* **1986**, *33*, 8800–8802, https://doi.org/10.1103/PhysRevB.33.8800
15. Koller, D.; Tran, F.; & Blaha, P. Merits and limits of the modified Becke-Johnson exchange potential. *Physical Review B* **2011**, *83*, 195134, https://doi.org/10.1103/PhysRevB.83.195134.
16. Ghaithan, H. M.; Alahmed, Z. A.; Qaid, S. M. H.; Hezam, M.; & Aldwayyan, A. S. Density Functional Study of Cubic, Tetragonal, and Orthorhombic $CsPbBr_3$ Perovskite. *ACS Omega* **2020**, *5*, 7468–7480, https://doi.org/10.1021/acsomega.0c00197.
17. Linaburg, M. R.; McClure, E. T.; Majher, J. D.; & Woodward, P. M. $Cs_{1-x}Rb_xPbCl_3$ and $Cs_{1-x}Rb_xPbBr_3$ Solid Solutions: Understanding Octahedral Tilting in Lead Halide Perovskites. *Chemistry of Materials* **2017**, *29*, 3507–3514, https://doi.org/10.1021/acs.chemmater.6b05372.
18. WIEN2k. Available online: http://susi.theochem.tuwien.ac.at/lapw/ (accessed on 1 May **2021**)
19. Materials Project. Available online: https://materialsproject.org/materials/mp-567681/ (accessed on 12 April **2021**)

20. López, C. A.; Abia, C.; Alvarez-Galván, M. C.; Hong, B.-K.; Martínez-Huerta, M. V.; Serrano-Sánchez, F.; Carrascoso, F.; Castellanos-Gómez, A.; Fernández-Díaz, M. T.; & Alonso, J. A. Crystal Structure Features of $CsPbBr_3$ Perovskite Prepared by Mechanochemical Synthesis. *ACS Omega* **2020**, *5*, 5931–5938, https://doi.org/10.1021/acsomega.9b04248.
21. Zhang, H.; Liu, X.; Dong, J.; Yu, H.; Zhou, C.; Zhang, B.; Xu, Y.; & Jie, W. Centimeter-Sized Inorganic Lead Halide Perovskite $CsPbBr_3$ Crystals Grown by an Improved Solution Method. *Crystal Growth & Design* **2017**, *17*, 6426–6431, https://doi.org/10.1021/acs.cgd.7b01086.
22. Protesescu, L.; Yakunin, S.; Bodnarchuk, M. I.; Krieg, F.; Caputo, R.; Hendon, C. H.; Yang, R. X.; Walsh, A.; & Kovalenko, M. v. Nanocrystals of Cesium Lead Halide Perovskites ($CsPbX_3$, X = Cl, Br, and I): Novel Optoelectronic Materials Showing Bright Emission with Wide Color Gamut. *Nano Letters* **2015**, *15*, 3692–3696, https://doi.org/10.1021/nl5048779.
23. Burschka, J.; Pellet, N.; Moon, S.-J.; Humphry-Baker, R.; Gao, P.; Nazeeruddin, M. K.; & Grätzel, M. Sequential deposition as a route to high-performance perovskite-sensitized solar cells. *Nature* **2013**, *499*, 316–319, https://doi.org/10.1038/nature12340.
24. Eperon, G. E.; Stranks, S. D.; Menelaou, C.; Johnston, M. B.; Herz, L. M.; & Snaith, H. J. Formamidinium lead trihalide: a broadly tunable perovskite for efficient planar heterojunction solar cells. *Energy & Environmental Science* **2014**, *7*, 982, https://doi.org/10.1039/c3ee43822h.
25. Zhang, J.; Hodes, G.; Jin, Z.; & Liu, S. (Frank). All-Inorganic $CsPbX_3$ Perovskite Solar Cells: Progress and Prospects. *Angewandte Chemie International Edition* **2019**, *58*, 15596–15618, https://doi.org/10.1002/anie.201901081.
26. Jiang, Y.; Yuan, J.; Ni, Y.; Yang, J.; Wang, Y.; Jiu, T.; Yuan, M.; & Chen, J. Reduced-Dimensional α-CsPbX3 Perovskites for Efficient and Stable Photovoltaics. *Joule* **2018**, *2*, 1356–1368, https://doi.org/10.1016/j.joule.2018.05.004. .
27. Stoumpos, C. C.; Malliakas, C. D.; & Kanatzidis, M. G. Semiconducting Tin and Lead Iodide Perovskites with Organic Cations: Phase Transitions, High Mobilities, and Near-Infrared Photoluminescent Properties. *Inorganic Chemistry* **2013**, *52*, 9019–9038, https://doi.org/10.1021/ic401215x.
28. Davlatshoevich, N. D. Investigation Optical Properties of the Orthorhombic System CsSnBr3-xIx: Application for Solar Cells and Optoelectronic Devices. *Journal of Human, Earth, and Future* **2021**, *2*, 404–411, https://doi.org/10.28991/HEF-2021-02-04-08.
29. Ahmad, M.; Rehman, G.; Ali, L.; Shafiq, M.; Iqbal, R.; Ahmad, R.; Khan, T.; Jalali-Asadabadi, S.; Maqbool, M.; & Ahmad, I. Structural, electronic and optical properties of CsPbX3 (X=Cl, Br, I) for energy storage and hybrid solar cell applications. *Journal of Alloys and Compounds* **2017**, *705*, 828–839, https://doi.org/10.1016/j.jallcom.2017.02.147.
30. Vickers, N. J. Animal Communication: When I'm Calling You, Will You Answer Too? *Current Biology* **2017**, *27*, R713–R715, https://doi.org/10.1016/j.cub.2017.05.064.
31. Yuan, Y.; Xu, R.; Xu, H.-T.; Hong, F.; Xu, F.; & Wang, L.-J. Nature of the band gap of halide perovskites ABX_3 (A = CH_3NH_3 , Cs; B = Sn, Pb; X = Cl, Br, I): First-principles calculations. *Chinese Physics B* **2015**, *24*, 116302, https://doi.org/10.1088/1674-1056/24/11/116302.
32. Zheng, Y.; Ouyang, M.; Han, X.; Lu, L.; & Li, J. Investigating the error sources of the online state of charge estimation methods for lithium-ion batteries in electric vehicles. *Journal of Power Sources* **2018**, *377*, 161–188, https://doi.org/10.1016/j.jpowsour.2017.11.094.
33. Rajeswarapalanichamy, R.; Amudhavalli, A.; Padmavathy, R.; & Iyakutti, K. Band gap engineering in halide cubic perovskites $CsPbBr_{3-y}I_y$ (y = 0, 1, 2, 3) – A DFT study. *Materials Science and Engineering: B* **2020**, *258*, 114560, https://doi.org/10.1016/j.mseb.2020.114560.
34. Murtaza, G.; & Ahmad, I. First principle study of the structural and optoelectronic properties of cubic perovskites $CsPbM_3$ (M=Cl, Br, I). *Physica B: Condensed Matter* **2011**, *406*, 3222–3229, https://doi.org/10.1016/j.physb.2011.05.028.
35. Nematov, D. Influence of Iodine Doping on the Structural and Electronic Properties of $CsSnBr_3$. *International Journal of Applied Physics* **2022**, *7*, https://www.iaras.org/iaras/home/caijap/influence-of-iodine-doping-on-the-structural-and-electronic-properties-of-cssnbr3.
36. Nematov, D. D.; Kholmurodov, K. T.; Husenzoda, M. A.; Lyubchyk, A.; & Burhonzoda, A. S. Molecular Adsorption of H_2O on TiO_2 and TiO_2: Y Surfaces. *Journal of Human, Earth, and Future* **2022**, *3*, 213-222, https://www.hefjournal.org/index.php/HEF/article/view/160.

37. Patel, M. J.; Raval, D.; Gupta, S. K.; & Gajjar, P. N. First-Principles Study of Mn-Doped and Nb-Doped $CsPbCl_3$ Monolayers as an Absorber Layer in Solar Cells. *The Journal of Physical Chemistry Letters* **2021**, *12*, 7319–7327, https://doi.org/10.1021/acs.jpclett.1c01100.
38. Nematov, D. D.; Kholmurodov, Kh. T.; Yuldasheva, D. A.; Rakhmonov, Kh. R.; & Khojakhonov, I. T. Ab-initio Study of Structural and Electronic Properties of Perovskite Nanocrystals of the $CsSn[Br_{1-x}I_x]_3$ Family. *HighTech and Innovation Journal* **2022**, *3*, 140–150, https://doi.org/10.28991/HIJ-2022-03-02-03.
39. Jing, X.; Zhou, D.; Sun, R.; Zhang, Y.; Li, Y.; Li, X.; Li, Q.; Song, H.; & Liu, B. Enhanced Photoluminescence and Photoresponsiveness of Eu^{3+} Ions-Doped $CsPbCl_3$ Perovskite Quantum Dots under High Pressure. *Advanced Functional Materials* **2021**, *31*, 2100930, https://doi.org/10.1002/adfm.202100930.
40. Rizwan, M.; Ayub, A.; Shakil, M.; Usman, Z.; Gillani, S. S. A.; Jin, H. B.; & Cao, C. B. Putting DFT to trial: For the exploration to correlate structural, electronic and optical properties of M-doped (M = Group I, II, III, XII, XVI) lead free high piezoelectric c-$BiAlO_3$. *Materials Science and Engineering: B* **2021**, *264*, 114959, https://doi.org/10.1016/j.mseb.2020.114959.
41. Kumari, A.; Nag, A.; & Kumar, J. Ab-initio study of halogen inter-substituted perovskite cesium lead halides for photovoltaic applications. *Journal of Physics and Chemistry of Solids* **2022**, *161*, 110430, https://doi.org/10.1016/j.jpcs.2021.110430.
42. Zhang, M.; Luo, Q.; Sheng, C.; Cao, D.; Chen, X.; & Shu, H. Space-confined growth of large-mismatch $CsPb(Br_xCI_{1-x})_3$ /GaN heterostructures with tunable band alignments and optical properties. *Inorganic Chemistry Frontiers* **2022**, *9*, 4661–4670, https://doi.org/10.1039/D2QI01039A.
43. Jing, X.; Sun, R.; Tian, H.; Liu, R.; Liu, B.; Zhou, D.; Li, Q.; & Liu, B. Evolution of self-trapped exciton emission tuned by high pressure in 2D all-inorganic cesium lead halide nanosheets. *Journal of Materials Chemistry C* **2022**, *10*, 8711–8718, https://doi.org/10.1039/D2TC01465C.
44. Ullah, S.; Yang, P.; Li, Y.; Wang, J.; Liu, L.; Mahmood, R.; Yang, S.-E.; Xia, T.; Guo, H.; & Chen, Y. Two step vapor-processing and experimental investigations of all-inorganic CsPbCl3 perovskite films for optoelectronic applications. *Materials Letters* **2021**, *294*, 129819, https://doi.org/10.1016/j.matlet.2021.129819.
45. Luo, D.; Yang, S.; Zhang, Q.; Cha, L.; Dang, L.; & Li, M.-D.. Precise Ligand Tuning Emission of Mn-Doped $CsPbCl_3$ Nanocrystals by the Amount of Sulfonates. *The Journal of Physical Chemistry Letters* **2021**, *12*, 1838–1846, https://doi.org/10.1021/acs.jpclett.1c00088.
46. Ayaz, U.; Shazia, Abdullah, Husain, M.; Rahman, N.; & Bonyah, E. *Ab initio* investigation of structural, electronic, magnetic, elastic, and optical properties of Cs-based chloro-perovskites $CsXCl_3$ (X = Be and Rh). *AIP Advances* **2021**, *11*, 105215, https://doi.org/10.1063/5.0065663.